

# Liquid–Liquid Equilibrium Measurements for Model Systems Related to Catalytic Fast Pyrolysis of Biomass

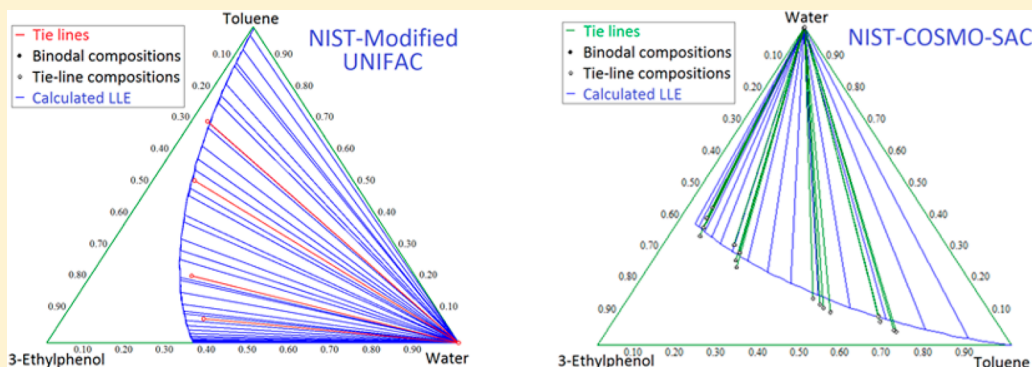
Louis V. Jasperson,<sup>\*,†</sup> Rubin J. McDougal,<sup>†</sup> Vladimir Diky,<sup>‡</sup> Eugene Paulechka,<sup>‡</sup> Robert D. Chirico,<sup>‡</sup> Kenneth Kroenlein,<sup>\*,‡</sup> Kristiina Iisa,<sup>§</sup> and Abhijit Dutta<sup>\*,§</sup>

<sup>†</sup>Wiltec Research Company, 488 S 500 W, Provo, Utah 84601-4226, United States

<sup>‡</sup>Thermodynamics Research Center, Applied Chemicals and Materials Division, National Institute of Standards and Technology, 325 Broadway, Boulder, Colorado 80305-3328, United States

<sup>§</sup>National Bioenergy Center, National Renewable Energy Laboratory, 15013 Denver West Parkway, Golden, Colorado 80401-3305, United States

## Supporting Information



**ABSTRACT:** We report liquid–liquid mutual solubilities for binary aqueous mixtures involving 2-, 3-, and 4-ethylphenol, 2-, 3-, and 4-methoxyphenol, benzofuran, and 1*H*-indene for the temperature range (300 < *T*/K < 360). Measurements in the water-rich phase for (2-ethylphenol + water) and (4-ethylphenol + water) were extended to *T* = 440 K and *T* = 380 K, respectively, to facilitate comparison with literature values. Liquid–liquid equilibrium tie-line determinations were made for four ternary systems involving (water + toluene) mixed with a third component: phenol, 3-ethylphenol, 4-methoxyphenol, or 2,4-dimethylphenol. Literature values at higher temperatures are available for the three (ethylphenol + water) systems, and in general, good agreement is seen. The ternary system (water + toluene + phenol) has been studied previously with inconsistent results reported in the literature, and one report is shown to be anomalous. All systems are modeled with the predictive methods NIST-modified-UNIFAC and NIST-COSMO-SAC, with generally good success (i.e., within 0.05 mole fraction) in the temperature range of interest (300 < *T*/K < 360). This work is part of a larger project on the testing and development of predictive phase equilibrium models for compound types occurring in catalytic fast pyrolysis of biomass, and background information for that project is provided.

## 1. INTRODUCTION

There is a current emphasis on developing conversion pathways for the production of renewable fuels and chemicals from lignocellulosic biomass materials, such as wood, corn stover, and wheat straw, that do not compete with food sources such as corn and sugar. In a simplistic representation, the primary constituents of lignocellulosic biomass are cellulose (a polysaccharide with glucose as building blocks), hemicellulose (a heteropolysaccharide with acetyl groups), lignin (an amorphous polyphenolic structure with variously bonded hydroxy and methoxy units), extractives (nonstructural organic matter of varying composition), and mineral matter (the inorganic content in biomass, often referred to as ash).<sup>1</sup> Thus, the primary atomic constituents are CHO, with varying amounts of other elements such as N and S, depending on

the biomass source. As an example, wood from some sources can be approximated by CH<sub>1.4</sub>O<sub>0.6</sub> (42 mass percent oxygen).<sup>1</sup>

The targeted products from biomass are often hydrocarbon fuels, necessitating deoxygenation of the biomass feedstock in the conversion processes.<sup>2,3</sup> In other cases the products contain oxygen (e.g., methanol and ethanol), which can be advantageous because some of the oxygen in the biomass—and its associated mass—is valued as part of the product.<sup>4,5</sup> Multiple pathways exist for the conversion of lignocellulosic biomass involving biochemical,<sup>6</sup> thermochemical,<sup>2,3,7</sup> and hybrid<sup>8,9</sup> methods. Biochemical or microorganism-based conversion is

Received: July 12, 2016

Accepted: October 13, 2016

naturally suited for the cellulose and hemicellulose in biomass<sup>6</sup> but has significant challenges in converting lignin.<sup>10</sup> Thermochemical conversion pathways can usually convert all the organic constituents, and gasification and pyrolysis are common processes. High-severity gasification processes, aided by oxygen or steam, typically operate in the 600–1500 °C (~900–1800 K) range.<sup>11</sup> The product is syngas, with simple molecules CO and H<sub>2</sub> as the desirable constituents. The syngas can be further converted to products, such as methanol, ethanol, dimethyl ether, and hydrocarbon fuels.<sup>12–15</sup> In contrast, pyrolysis typically involves the heating of biomass in the absence of oxygen at lower temperatures, leading to a partial breakdown of the biomass. The pyrolysis products retain the signatures of the native constituents of the biomass, albeit in the form of depolymerized and fragmented compounds. A specific type of pyrolysis, called *fast pyrolysis* (FP), is conducted at approximately 500 °C (~800 K) with short vapor residence times of ~2 s, giving the highest yields of condensable products (also known as bio-oil or pyrolysis oil upon condensation),<sup>1</sup> while minimizing undesirable noncondensable gases and solid char. However, the bio-oil is reactive, unstable, and acidic because it still retains significant oxygen from the biomass and has limited direct applications<sup>16</sup> but can be further hydroprocessed to fungible liquid hydrocarbon fuels.<sup>2</sup> During FP, deoxygenation of the liquid product occurs primarily with the formation of H<sub>2</sub>O, CO, and CO<sub>2</sub>; the H<sub>2</sub>O, as expected, remains in the liquid bio-oil and is produced in significant quantities.<sup>16</sup>

*Catalytic fast pyrolysis* (CFP) involves the use of catalysts to improve the vapor quality by further reducing the oxygen content, thus producing a more stable bio-oil.<sup>17–19</sup> The catalyst may be present within the FP reactor (*in situ*) or in a separate reactor following the FP reactor (*ex situ*). Some of the processing implications of these configurations have been discussed in the literature.<sup>3,20</sup>

The focus of this article is on the liquid–liquid equilibrium (LLE) behavior of model compounds for the condensed products from CFP. The heterogeneous and varied structure of biomass is reflected in the reaction products of FP, where compounds number in the thousands<sup>21</sup> and complete speciated quantification is not achieved for FP derived bio-oil.<sup>1</sup> Bio-oil from FP includes a wide range of molecular weights and a variety of oxygenated functional groups.<sup>22</sup> The compounds from CFP are often more tractable because deoxygenation reduces the number and abundance of oxygenated species,<sup>23</sup> and some shape-selective catalysts such as zeolites narrow the molecular weight ranges and compounds in the products.<sup>24</sup> The degree of catalytic deoxygenation and associated reduction in the polarity of species can result in different LLE separation behavior of bio-oils. The oxygen-content range is broad, from 40% in noncatalytic processes<sup>16</sup> to less than 10% in significantly deoxygenated oils.<sup>19</sup> There is usually an economic optimum during deoxygenation for any specific process/catalyst, because typically higher deoxygenation—resulting in better quality—is associated with lower carbon efficiency, translating to lower product yields.

The emphasis of this project is on the testing and development of predictive phase equilibrium models, with initial focus on LLE. Predictive models are emphasized because of the diverse compositions of differently produced bio-oils and the futility of trying to experimentally generate binary data for every possible compound pair. Nonetheless, the model development needs to be informed and validated with key

experimental data, which is the reason for supplementing existing literature information with targeted experiments here.

Liquid–liquid separation is a key process in the downstream processing of bio-oil. While FP bio-oil (without catalytic upgrading) typically remains in a single phase until the proportion of water increases (see Figure 3 in ref 22), deoxygenated oils from CFP tend to spontaneously separate into organic and aqueous phases. The separation often results in an aqueous phase sandwiched between light and heavy organic phases,<sup>25</sup> again depending on molecular weight ranges and the degree of deoxygenation. Studies of processing strategies and their optimization can be significantly improved by understanding LLE behavior and separations in such systems. In addition, this understanding can influence wastewater handling and the utilization of carbon otherwise lost in the aqueous phase. Models found to be effective in this work can be applied to other biomass processes because almost all biomass conversion involves oxygenated species. LLE of bio-oil from pyrolysis processes, especially the ones with lower deoxygenation, are however some of the most challenging to model because of the variety of compounds and low selectivity toward any specific compound.

This work was initiated by selecting a subset of compounds (as model compounds) from CFP experiments at NREL. Experimental and analytical methods for the CFP experiments are described in detail by Iisa et al.<sup>25</sup> Identified compounds were classified into the following categories: 1-ring aromatics, naphthalenes, indanes/indenes, 3- and 4-ring aromatics, light oxygenates, furans, phenols, methoxyphenols, indenols and naphthenols, cyclopentenones, and anhydrosugars. For our initial LLE experiments, involving only a small subset of those compounds, the selections were driven primarily by the representation of key functional groups and data availability in the literature. The effects of the relative positions of alkyl (methyl and ethyl) and methoxy and hydroxy groups in the aromatic structure were given priority because of their importance in model development.

Based on the CFP analytical results,<sup>25</sup> a set of model compounds and model systems were selected for measurement. The three ethylphenols were selected because some experimental LLE were available in the literature, but mostly from a single source published in 1955 (Terres et al.),<sup>26</sup> where LLE of numerous substituted phenols with water had been reported. If consistency could be demonstrated between the present earlier results, a significant portion of the literature for (water + phenolic) systems would be validated. The three methoxy phenols, benzofuran, and 1H-indene were selected because of their relatively large representation in the analytical results combined with an absence of LLE data with water in the literature. Toluene was selected to represent the organic phase in the ternary studies because the analytical results<sup>25</sup> showed organic products to be largely single aromatic rings with short side chains, for which toluene is the prototype. Mutual solubilities for the system (water + toluene) have been studied extensively and were most recently reviewed by Maczynski et al.<sup>27</sup> In this research, ternary systems involving (water + toluene) were studied in the temperature range 300–360 K. Evaluated solubilities of toluene in water and water in toluene are 0.0002 mole fraction and 0.015 mole fraction, respectively, at  $T = 360$  K. Critically evaluated<sup>27</sup> solubilities for (water + toluene) for all temperatures of this research are listed in Table S1 in the Supporting Information. A review of the existing literature of LLE studies involving water with other compounds

Table 1. Source and Purity of Chemical Samples

chemical name	CAS RN <sup>a</sup>	source <sup>b</sup>	purification method <sup>c</sup>	mass fraction purity
2-ethylphenol	90-00-6	ChemSampCo	none	0.960
3-ethylphenol	620-17-7	Alfa Aesar	none	0.961 <sup>d</sup>
4-ethylphenol	123-07-9	TCI America	none	0.987
2-methoxyphenol	90-05-1	TCI America	none	0.998
3-methoxyphenol	150-19-6	Sigma-Aldrich	none	0.983
4-methoxyphenol	150-76-5	TCI America	none	0.994
2,4-dimethylphenol	105-67-9	TCI America	none	0.990
phenol	108-95-2	Sigma-Aldrich	none	0.999
toluene	108-88-3	Sigma-Aldrich	none	0.999
benzofuran	271-89-6	Alfa Aesar	none	0.993
1 <i>H</i> -indene	95-13-6	ChemSampCo	none	0.963
water	7732-18-5	AquaOne	none	0.999

<sup>a</sup>Chemical Abstracts Service Registry Number. <sup>b</sup>Web sites for chemical suppliers: [www.chemsampco.com](http://www.chemsampco.com), [www.alfa.com](http://www.alfa.com), [www.tcichemicals.com](http://www.tcichemicals.com), [www.sigmaldrich.com](http://www.sigmaldrich.com), [www.drinkaquaone.com](http://www.drinkaquaone.com). <sup>c</sup>All samples were degassed in the measurement cell before equilibration. <sup>d</sup>Mass fraction impurities in the 3-ethylphenol sample were 2.1% 4-ethylphenol, 1.1% phenol, 0.18% water, 0.1% *m*-cresol, plus other trace compounds, as determined by the supplier.

studied here did reveal some previous relevant results, but these were often at temperatures in excess of those of interest in the present research ( $T < 100$  °C (373 K))<sup>26,28,29</sup> or were mutually inconsistent.<sup>30,31</sup>

Two predictive methods were recently reparameterized at NIST, NIST-COSMO-SAC<sup>32</sup> and NIST-modified-UNIFAC,<sup>33</sup> and both were applied to all measured systems. The original bridge between empirical models and quantum chemistry was COSMO-RS (Conductor-like Screening Model for Real Solvents), as formulated by Klamt et al.<sup>34,35</sup> Subsequent to this work, alternative approaches have been developed (e.g., COSMO-RS(OI),<sup>36</sup> COSMORS(ADF),<sup>37</sup> COSMO-SAC,<sup>38</sup> COSMO-3D<sup>39</sup>). Comparisons of performance levels<sup>40,41</sup> for COSMO-RS, COSMO-RS(OI), and COSMO-SAC showed that results were similar for the various methods. In the development of NIST-COSMO-SAC,<sup>32</sup> the temperature-dependent  $\sigma$  profiles included contributions of up to 40 conformers for a molecule. Also, splitting of the H-bonding  $\sigma$  profiles into OH and non-OH parts decreased the root-mean-square deviation from the experimental data points by ~10% relative to the model using one H-bonding parameter. This refinement is particularly important in the present research, where water and phenolic compounds are major components.

NIST-modified-UNIFAC<sup>33</sup> is based on the modified UNIFAC model formulated by Gmehling and co-workers.<sup>42–46</sup>

The modified UNIFAC model provides improved property prediction through additional temperature-dependent terms in the representation of interaction parameters. All UNIFAC methods are empirically parameterized with experimental data, so if data are unavailable or unreliable for certain groups, no predictions can be made. Parameterization of the COSMO method involves the evaluation of sigma profiles derived from computational chemistry, so limitations caused by lack of experimental data are avoided. Predictions made with NIST-modified UNIFAC and NIST-COSMO-SAC are compared with experimental results obtained for all mixtures in this research, and their relative effectiveness is discussed.

## 2. MATERIALS AND METHODS

**2.1. Materials.** All chemical samples used in this study were obtained from commercial suppliers and used without further purification. The chemical name, Chemical Abstracts Service Registry Number (CASRN), supplier, and the purity stated by

the supplier, are listed for each chemical in Table 1. Three compounds (2-ethylphenol, 3-ethylphenol, and indene) have relatively low purities near 0.96 mass fraction. For 3-ethylphenol, analysis by the supplier showed that the major impurity was 4-ethylphenol.

**2.2. Measurements.** LLE measurements were obtained with the apparatus shown schematically in Figure 1. This

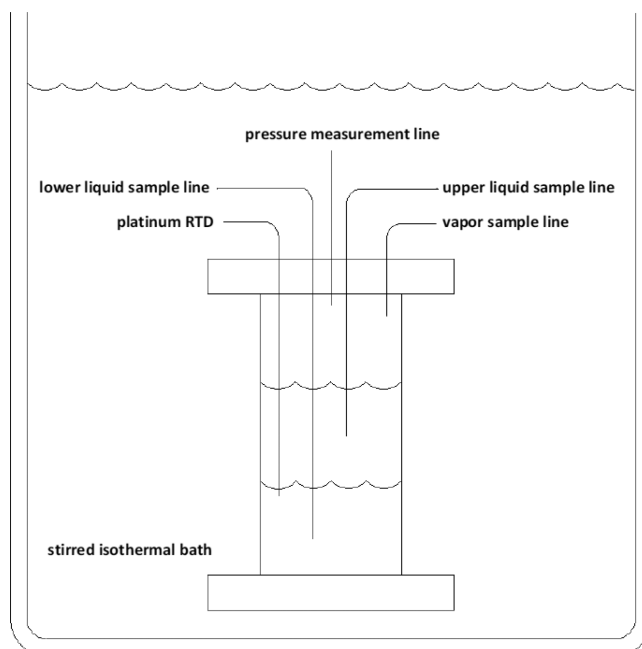


Figure 1. Schematic of the experimental setup for the LLE measurements.

apparatus consists of a 300 cm<sup>3</sup> glass cylinder with stainless steel flanges bolted together as end caps. The cell flanges were sealed to the glass cylinder with polytetrafluoroethylene (PTFE) O-rings. The cell was equipped with lines for sampling of each phase, plus sample charging and degassing. The vapor sample line was not used in the present study. The liquid in the cell was stirred with a Teflon-coated magnetic stir bar. The temperature of the mixture in the cell was measured with a standard uncertainty of 0.02 K with a platinum resistance

**Table 2. Experimental Liquid–Liquid Equilibrium Mole Fractions  $x$  for Binary Systems at Temperatures  $T$  and Pressure  $p = 0.085$  MPa<sup>a</sup>**

T/K	aqueous phase		organic phase			T/K	aqueous phase		organic phase		
	$x_1'$	$u(x_1')$	$x_1''$	$u(x_1'')$	Loc <sup>b</sup>		$x_1'$	$u(x_1')$	$x_1''$	$u(x_1'')$	Loc <sup>b</sup>
2-Ethylphenol (1) + Water (2)											
300.0	0.0018	0.0001	0.642	0.009	B	300.0	0.0060	0.0002	0.764	0.006	B
320.0	0.0019	0.0001	0.622	0.006	B	320.0	0.0056	0.0003	0.741	0.005	B
340.0	0.0022	0.0001	0.593	0.006	T	340.0	0.0062	0.0003	0.703	0.006	B
360.0	0.0029	0.0001	0.570	0.018	T	360.0	0.0080	0.0005	0.688	0.009	B
380.0	not measured		0.540	0.011	T						
400.0	not measured		0.513	0.004	T						
420.0	not measured		0.477	0.004	T						
440.0	not measured		0.413	0.006	T						
3-Ethylphenol (1) + Water (2)											
300.0	0.0034	0.0001	0.600	0.001	B	300.0	0.0097	0.0001	0.400	0.019	B
320.0	0.0021	0.0001	0.580	0.001	T	320.0	0.0100	0.0004	0.371	0.003	B
340.0	0.0026	0.0001	0.535	0.005	T	340.0	0.0129	0.0003	0.319	0.013	B
360.0	0.0030	0.0001	0.502	0.011	T	360.0	0.0226	0.0009	0.274	0.008	B
4-Ethylphenol (1) + Water (2)											
300.0	0.0025	0.0001	0.515	0.022	B	300.0	0.0127	0.0003	0.4171	0.0005	B
320.0	0.0017	0.0001	0.490	0.022	T	320.0	0.0158	0.0011	0.3840	0.0004	B
340.0	0.0019	0.0001	0.474	0.014	T	340.0	0.0216	0.0014	0.3238	0.0125	B
360.0	0.0031	0.0002	0.448	0.002	T	360.0	0.0329	0.0008	0.2575	0.0027	B
380.0	not measured		0.416	0.005	T						
Benzofuran (1) + Water (2)											
300.0	0.00023	0.00002	0.9905	0.0003	B	300.0	0.00004	0.00001	0.9942	0.0001	T
320.0	0.00021	0.00002	0.9855	0.0002	B	320.0	0.00009	0.00001	0.9905	0.0003	T
340.0	0.00026	0.00002	0.9772	0.0009	B	340.0	0.00010	0.00001	0.9851	0.0001	T
360.0	0.00035	0.00002	0.9663	0.0002	B	360.0	0.00014	0.00001	0.9766	0.0003	T

<sup>a</sup>The standard uncertainties are  $u(T) = 0.02$  K and  $u(p) = 0.003$  MPa. Standard uncertainties for the measured compositions  $u(x)$  are given in the body of the table. <sup>b</sup>B (bottom) and T (top) indicate the location of the organic phase in the two-phase mixture.

thermometer inserted into a thermowell in the top of the cell. Bath and cell thermometers were calibrated using ice and steam points and referenced to a NIST traceable standard resistance thermometer.

Measurements were initiated by evacuation and charging of the cell with the desired amounts of each compound. Approximately one-half of the cell volume was filled with liquid. For the binary systems, 60–70 g of each component were used, while for the ternary systems, 40–50 g of each component were loaded into the measurement cylinder. For some measurements on ternary systems, a larger proportion of one component was added to ensure that the upper liquid sample line was in the upper liquid phase (Figure 1). The cell was placed in the constant temperature bath, and the bath was brought to the desired temperature. The cell contents were vigorously stirred for a minimum of 15 min, and the phases were allowed to come to equilibrium. The stirrer was then shut off, and the liquid phases were allowed to settle. Settling times were dependent on the particular mixture, and samples were allowed to settle for a minimum of 15 min after visual observation of separation. Several mixtures required overnight for the phases to separate. Samples were collected over at least 1 h and frequently several hours, enabling a determination of the compositions over an extended time period without any detectable shift in the results, thus assuring that equilibrium had been reached. Sampling was accomplished by pressurizing the cell to 0.15–0.3 MPa with dry nitrogen. Multiple samples of the upper liquid and lower liquid phases were withdrawn into weighed vials.

Sample vials for the aqueous phase contained 1-propanol to assist in solvation and to act as an internal standard. Samples of the aqueous phase were analyzed with an HP 5890 gas chromatograph fitted with a Supelco SAC-5 column. The column was 30 m long with an internal bore diameter of 0.25 mm and 0.25  $\mu$ m film thickness. The gas chromatograph was operated isothermally at 150 °C (423 K) with the temperatures of the injection port and flame ionization detector held constant at 250 °C (523 K). Typical retention times for the oxygenates were approximately 2.5 min. Water content in samples of the organic phase was analyzed using a Mettler Toledo DL31 Karl Fischer titrator. For ternary systems containing toluene, additional samples were taken from the organic phase and analyzed by gas chromatograph. Phase analyses were typically based on four samples of mass 0.3–1.0 g, with each sample analyzed a minimum of eight times. Mole fraction compositions  $x$  were determined with a relative standard uncertainty  $u_r(x) \approx 0.02$ , based on the standard deviation for roughly 30 determinations. Low toluene concentrations in the aqueous phase proved difficult to analyze, and the reported uncertainties reflect this, with  $u_r(x) \approx 15\%$ . Standard uncertainties for individual compositions are given in the tables of results (Tables 2 and 3).

### 3. RESULTS AND DISCUSSION

**3.1. Experimental Results.** Results of the LLE measurements are listed in Table 2 for the eight binary systems and Table 3 for the four ternary systems. The location of the organic phase (top or bottom) is also noted for all mixtures in the tables. For the binary systems, inversions were observed for

Table 3. Experimental Tie-Line Mole Fractions  $x$  for Ternary Systems at Temperatures  $T$  and Pressure  $p = 0.085$  MPa<sup>a</sup>

T/K	aqueous phase					organic phase					Loc <sup>b</sup>
	$x_1'$	$u(x_1')$	$x_2'$	$u(x_2')$	$x_1''$	$u(x_1'')$	$x_2''$	$u(x_2'')$			
4-Methoxyphenol (1) + Toluene (2) + Water (3)											
300.0	0.0069	0.0002	0.00007	0.00001	0.454	0.002	0.061	0.003		B	
300.0	0.0070	0.0001	0.00016	0.00004	0.393	0.007	0.304	0.008		B	
300.0	0.0055	0.0001	0.00010	0.00001	0.264	0.005	0.627	0.005		T	
300.0	0.0060	0.0003	0.00005	0.00001	0.145	0.004	0.816	0.004		T	
320.0	0.0096	0.0005	0.00013	0.00001	0.420	0.001	0.058	0.001		B	
320.0	0.0083	0.0002	0.00009	0.00003	0.404	0.003	0.266	0.003		B	
320.0	0.0070	0.0004	0.00009	0.00003	0.260	0.005	0.623	0.006		T	
320.0	0.0050	0.0002	0.00005	0.00001	0.174	0.012	0.781	0.012		T	
340.0	0.0133	0.0003	0.00014	0.00001	0.388	0.001	0.050	0.001		B	
340.0	0.0105	0.0002	0.00014	0.00001	0.408	0.009	0.226	0.010		B	
340.0	0.0097	0.0004	0.00011	0.00001	0.286	0.007	0.580	0.007		T	
340.0	0.0057	0.0002	0.00017	0.00001	0.158	0.008	0.789	0.008		T	
360.0	0.0195	0.0002	0.00025	0.00001	0.344	0.001	0.043	0.001		B	
360.0	0.0130	0.0005	0.00022	0.00001	0.382	0.003	0.226	0.003		B	
360.0	0.0138	0.0002	0.00023	0.00002	0.288	0.004	0.556	0.004		T	
360.0	0.0091	0.0003	0.00019	0.00004	0.149	0.008	0.788	0.008		T	
3-Ethylphenol (1) + Toluene (2) + Water (3)											
300.0	0.0014	0.0001	0.00011	0.00001	0.579	0.003	0.078	0.003		T	
300.0	0.0015	0.0001	0.00012	0.00001	0.541	0.005	0.213	0.006		T	
300.0	0.0012	0.0001	0.00010	0.00001	0.384	0.013	0.514	0.014		T	
300.0	0.0008	0.0001	0.00005	0.00002	0.258	0.009	0.701	0.009		T	
320.0	0.0015	0.0001	0.00011	0.00001	0.557	0.002	0.072	0.003		T	
320.0	0.0016	0.0001	0.00013	0.00001	0.532	0.005	0.202	0.006		T	
320.0	0.0013	0.0001	0.00011	0.00001	0.396	0.010	0.488	0.010		T	
320.0	0.0009	0.0001	0.00008	0.00001	0.260	0.009	0.694	0.009		T	
340.0	0.0029	0.0001	0.00018	0.00001	0.536	0.003	0.065	0.004		T	
340.0	0.0020	0.0001	0.00015	0.00001	0.510	0.006	0.198	0.006		T	
340.0	0.0015	0.0001	0.00012	0.00003	0.398	0.011	0.473	0.012		T	
340.0	0.0011	0.0001	0.00009	0.00001	0.279	0.011	0.648	0.011		T	
360.0	0.0031	0.0001	0.00019	0.00001	0.505	0.002	0.063	0.002		T	
360.0	0.0023	0.0001	0.00017	0.00001	0.510	0.004	0.176	0.004		T	
360.0	0.0016	0.0001	0.00012	0.00001	0.405	0.013	0.448	0.014		T	
360.0	0.0014	0.0001	0.00007	0.00002	0.275	0.010	0.636	0.010		T	
Phenol (1) + Toluene (2) + Water (3)											
300.0	0.0182	0.0005	0.00005	0.00001	0.404	0.002	0.033	0.002		B	
300.0	0.0152	0.0005	0.00007	0.00002	0.441	0.004	0.140	0.004		B	
300.0	0.0104	0.0002	0.00005	0.00001	0.371	0.004	0.466	0.004		T	
300.0	0.0081	0.0001	0.00005	0.00001	0.230	0.005	0.706	0.005		T	
320.0	0.0208	0.0001	0.00006	0.00001	0.368	0.002	0.030	0.002		B	
320.0	0.0156	0.0001	0.00019	0.00004	0.426	0.002	0.127	0.002		T	
320.0	0.0113	0.0002	0.00005	0.00001	0.349	0.008	0.476	0.008		T	
320.0	0.0088	0.0002	0.00010	0.00002	0.224	0.003	0.706	0.003		T	
340.0	0.0234	0.0004	0.00012	0.00003	0.366	0.003	0.046	0.004		B	
340.0	0.0200	0.0003	0.00015	0.00004	0.402	0.005	0.114	0.005		T	
340.0	0.0134	0.0006	0.00009	0.00001	0.357	0.013	0.452	0.013		T	
340.0	0.0092	0.0001	0.00016	0.00001	0.215	0.004	0.704	0.004		T	
360.0	0.0322	0.0011	0.00032	0.00006	0.298	0.002	0.046	0.002		T	
360.0	0.0252	0.0008	0.00023	0.00006	0.367	0.002	0.103	0.002		T	
360.0	0.0159	0.0003	0.00017	0.00003	0.362	0.005	0.421	0.005		T	
360.0	0.0104	0.0001	0.00010	0.00001	0.208	0.008	0.698	0.008		T	
2,4-Dimethylphenol (1) + Toluene (2) + Water (3)											
300.0	0.0021	0.0001	0.00015	0.00004	0.591	0.001	0.068	0.001		B	
300.0	0.0011	0.0001	0.00007	0.00003	0.549	0.012	0.228	0.013		T	
300.0	0.0007	0.0001	0.00007	0.00001	0.351	0.003	0.564	0.003		T	
300.0	0.0005	0.0001	0.00013	0.00002	0.212	0.013	0.751	0.013		T	
320.0	0.0015	0.0001	0.00016	0.00003	0.567	0.001	0.075	0.001		T	
320.0	0.0016	0.0001	0.00007	0.00001	0.543	0.002	0.219	0.002		T	
320.0	0.0007	0.0001	0.00017	0.00002	0.361	0.006	0.545	0.006		T	

Table 3. continued

T/K	aqueous phase					organic phase					Loc <sup>b</sup>
	$x_1'$	$u(x_1')$	$x_2'$	$u(x_2')$	$x_1''$	$u(x_1'')$	$x_2''$	$u(x_2'')$			
2,4-Dimethylphenol (1) + Toluene (2) + Water (3)											
320.0	0.0005	0.0001	0.00019	0.00005	0.207	0.015	0.751	0.016		T	
340.0	0.0025	0.0002	0.00005	0.00001	0.561	0.003	0.072	0.003		T	
340.0	0.0013	0.0001	0.00006	0.00001	0.558	0.007	0.193	0.007		T	
340.0	0.0010	0.0001	0.00007	0.00003	0.344	0.008	0.553	0.008		T	
340.0	0.0006	0.0001	0.00010	0.00002	0.228	0.005	0.724	0.005		T	
360.0	0.0027	0.0002	0.00006	0.00001	0.545	0.001	0.068	0.001		T	
360.0	0.0018	0.0002	0.00007	0.00002	0.541	0.013	0.196	0.014		T	
360.0	0.0010	0.0001	0.00010	0.00003	0.348	0.011	0.534	0.011		T	
360.0	0.0007	0.0001	0.00008	0.00002	0.244	0.010	0.697	0.010		T	

<sup>a</sup>The standard uncertainties are  $u(T) = 0.02$  K and  $u(p) = 0.003$  MPa. Standard uncertainties for the measured compositions  $u(x)$  are given in the body of the table. <sup>b</sup>B (bottom) and T (top) indicate the location of the organic phase in the two-phase mixture.

mixtures of 2-, 3-, and 4-ethylphenol with water. For the ternary mixtures, only the system (3-ethylphenol + toluene + water) did not invert at any temperature or composition.

**3.2. Comparisons with Literature Data.** Of the eight binary systems investigated, only those involving the ethylphenols were studied previously. Terres et al.<sup>26</sup> measured LLE temperatures for an extensive series of alkyl-substituted phenols with water, including 2-ethylphenol ( $T = 410$ –487 K), 3-ethylphenol ( $T = 385$ –463 K), and 4-ethylphenol ( $T = 376$ –455 K). The system (4-ethylphenol + water) was also studied by Erichsen and Dobbert<sup>28</sup> ( $T = 433$ –486 K). Figure 2 shows comparisons of the literature data with those of this research for

each (ethylphenol + water) system. As seen in Figure 2, agreement is good for all data and systems, except for a single value reported by Terres et al.<sup>26</sup> for (2-ethylphenol + water), as shown in the figure. We extended the measurements of this research to  $T = 440$  K for this system to test if consistency was achieved at higher temperatures, and it was.

Of the four ternary systems studied here, LLE have previously been reported for one system, (phenol + toluene + water). Martin et al.<sup>31</sup> reported binodal data at the temperature  $T = 298$  K. Tie-lines were reported by Mohsen-Nia and Paikar<sup>30</sup> ( $T = 298.15$  and 303.15 K) and Hooper et al.<sup>29</sup> ( $T = 423$  and 473 K). Literature data near  $T = 300$  K are compared with those of the present research in Figure 3. Agreement with the binodal data of Martin et al.<sup>31</sup> is within 0.03 mole fraction, while results reported by Mohsen-Nia and Paikar<sup>30</sup> (shown in red) are seen to be anomalous. The high-temperature values reported by Hooper et al.<sup>29</sup> are not shown for clarity, but these are consistent with expected trends in

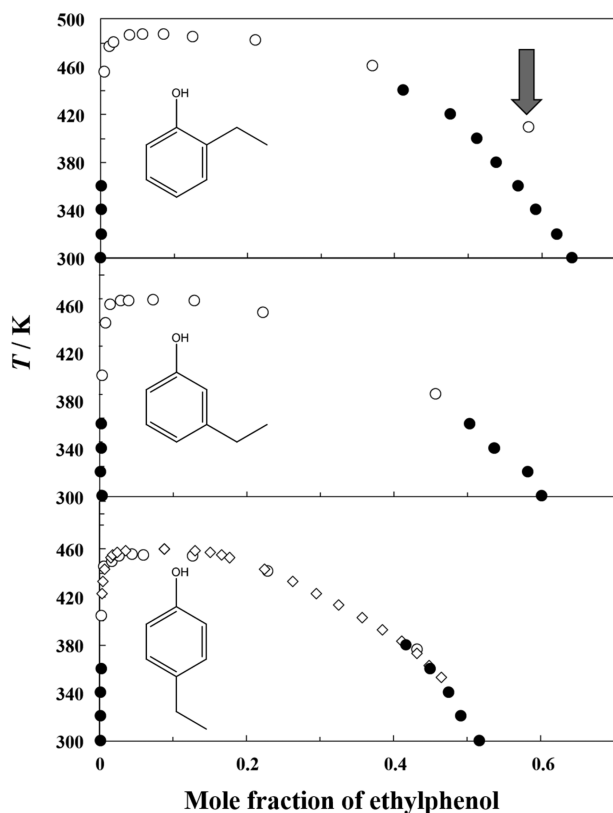


**Figure 2.** Comparisons with literature LLE data for the (ethylphenol + water) systems at pressure  $p = 0.08_5$  MPa. ○, Terres et al.; <sup>26</sup> ◇, Erichsen and Dobbert; <sup>28</sup> ●, this research. The arrow indicates the single anomalous value reported by Terres et al.<sup>26</sup>

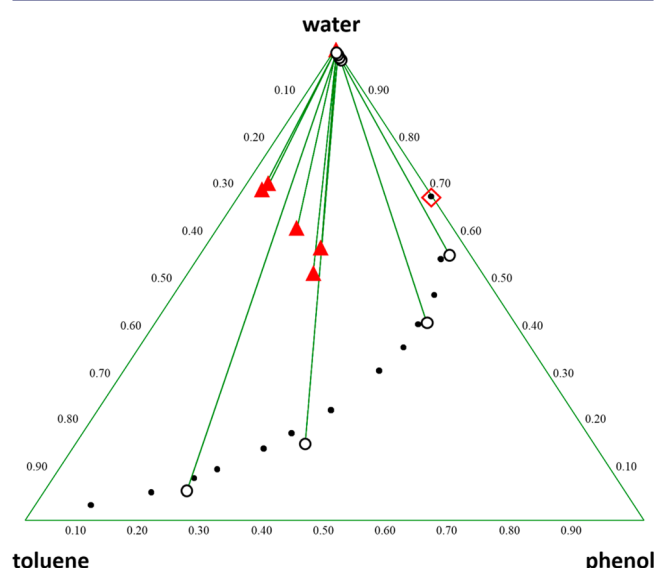


**Figure 3.** Comparison with literature LLE data for the system (phenol + toluene + water) near  $T/K = 300$  K and pressure  $p = 0.08_5$  MPa. ●, Martin et al.<sup>31</sup> (binodal data at  $T/K = 298.15$  K); red ▲, Mohsen-Nia and Paikar<sup>30</sup> (tie-line data at  $T/K = 298.15$  K); ○, this research (tie-line data at  $T = 298.15$  K). Tie-line data are connected with the green lines. Red ◇, LLE composition at  $T = 300$  K for the binary system (phenol + water) evaluated by Goral et al.<sup>47</sup>

solubility with temperature, as well as with the predictive models used here. The binary system (phenol + water) has been studied extensively, and the LLE composition at  $T = 300$  K evaluated by Goral et al.<sup>47</sup> is included in Figure 3.

**3.3. Comparisons with Predictive Models.** The NIST-modified-UNIFAC and NIST-COSMO-SAC models were applied to the eight binary and four ternary systems studied. For the binary systems, both models are in fair accord with the experimental data near  $T = 300$  K but deviate high near the consolute composition. A typical result is shown in Figure 4,

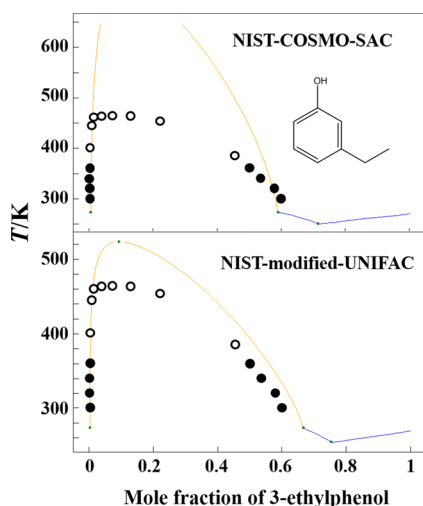


**Figure 4.** Comparison of results from predictive models with experimental LLE data for the binary system (3-ethylphenol + water) at pressure  $p = 0.085$  MPa. ○, Terres et al.; ●, this research. The orange lines represent the region of predicted liquid–liquid equilibrium, and the blue lines represent predicted solid–liquid equilibrium. The green dots represent transitions between the various types of predicted phase equilibrium.

where experimental data of this research and the literature are compared with both predictive models. Similar comparisons are provided for all systems in the *Supporting Information* for this article.

For the binary systems, agreement between the experimental and predicted data for both prediction methods is similar. A notable exception is the system (2-methoxyphenol + water), for which results are shown in Figure 5. Here, the NIST-modified-UNIFAC method overestimates the solubility of water in 2-methoxyphenol by ~0.2 mole fraction. In contrast, the prediction with NIST-COSMO-SAC shows good agreement (within 0.03 mole fraction) with the experimental values. A possible explanation for this result highlights a key difference between the NIST-modified-UNIFAC and COSMO methods. For the NIST-modified-UNIFAC, group definitions result in ortho, meta, and para substitutions being treated identically, while for COSMO—which is based on computed charge distributions for each molecule—this limitation does not exist. The 2-methoxyphenol molecule may include an intramolecular hydrogen bond between the oxygen of the  $-\text{OCH}_3$  group and the  $-\text{OH}$  group that could result in a reduced the strength of interaction with water, resulting in a lower solubility of water relative to that in the meta and para isomers. To account for this, a special ortho  $\text{OH}$ – $\text{O}$  group contribution would need to be added to the NIST-modified-UNIFAC method. This argument is supported by the fact that no analogous reduction in water solubility is seen in 2-ethylphenol relative to 3- and 4-

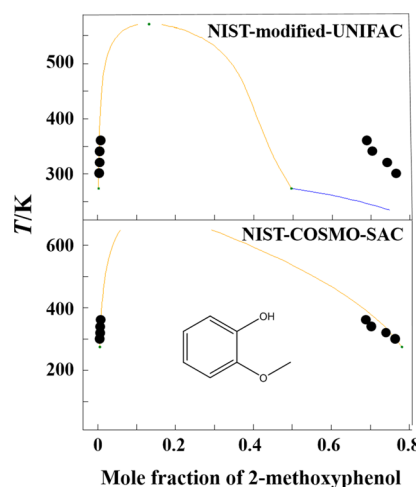


**Figure 5.** Comparison of results from predictive models with experimental LLE data for the binary system (2-methoxyphenol + water) at pressure  $p = 0.085$  MPa. ●, this research. The orange lines represent the region of predicted liquid–liquid equilibrium, and the blue lines represent predicted solid–liquid equilibrium. The green dots represent transitions between the various types of predicted phase equilibrium.

ethylphenol, implying that the reduced solubility in 2-methoxyphenol is not due simply to ortho substitution. A general argument cannot be made based on a single example, and a more extensive comparative review of the two prediction methods is justified. This is planned as part of future work.

For ternary systems, predictions made with NIST-modified-UNIFAC and NIST-COSMO-SAC are similar for all systems, with good agreement between prediction and experiment for all temperatures  $T = 300$ –360 K and compositions, with mole-fraction deviations, generally, well within 0.05 mole fraction. Typical results are shown in Figure 6 for the system (toluene + 2,4-dimethylphenol + water) at the temperature  $T = 320$  K. Analogous plots for all ternary systems at all temperatures are given in the *Supporting Information*.

**3.4. Comparison with Literature Data for the System (2,4-Dimethylphenol + Water).** In Figure 6, there is an inconsistency between the ternary data for the system (2,4-dimethylphenol + toluene + water) (●, this research) and literature values for the binary system (2,4-dimethylphenol + water) (red ♦) reported by Terres et al.<sup>26</sup> The LLE data of Terres et al.<sup>26</sup> are shown in Figure 7, together with values reported by Erichsen and Dobbert<sup>28</sup> and estimated values obtained in this research by graphical extrapolation of the ternary data to the binary limit. Values obtained in these extrapolations are shown in Figure 7 (symbol ×) and in the ternary diagrams for the system (2,4-dimethylphenol + toluene + water) provided in the *Supporting Information* (Figures S21–S24). The dashed line in Figure 7 was used, here, to calculate values based on the results of Terres et al.<sup>26</sup> at the temperatures of our research.

It is clear in Figure 7 that the results of Terres et al.<sup>26</sup> and Erichsen and Dobbert<sup>28</sup> begin to diverge near 0.3 mole fraction. Erichsen and Dobbert<sup>28</sup> did not report results for temperatures less than  $T = 440$  K for the organic-rich phase, so extrapolation to the conditions of the present research ( $T = 300$ –360 K) cannot be done with any confidence. While it is tempting to declare consistency between the present research and the work of Erichsen and Dobbert<sup>28</sup> the large temperature gap seen in

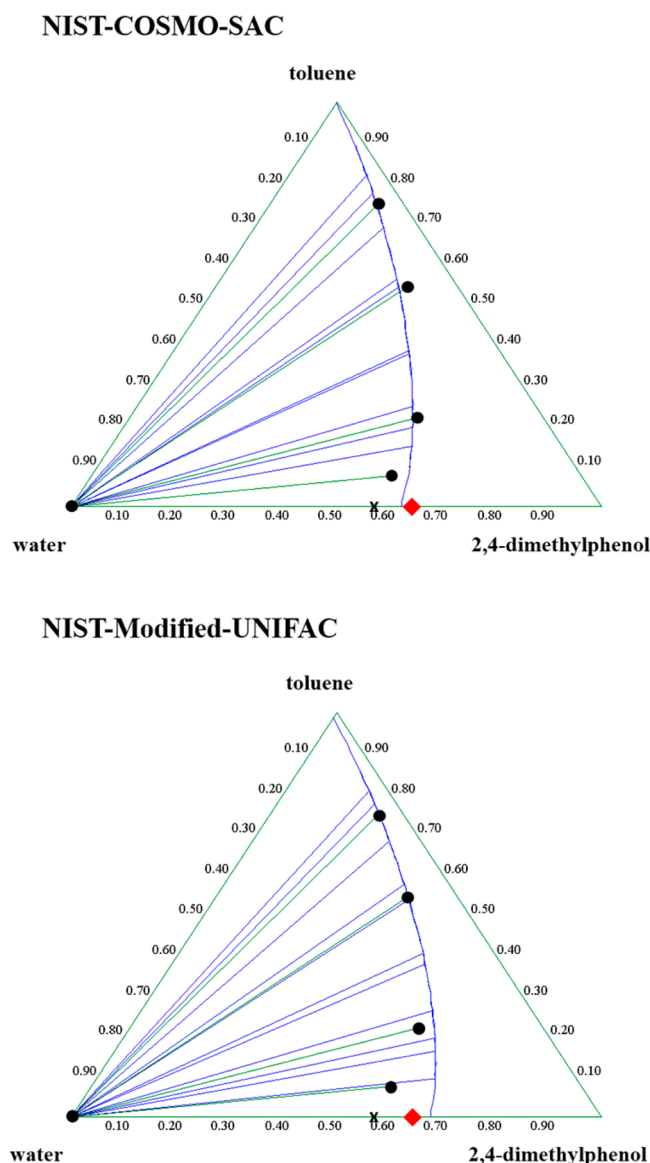


**Figure 6.** Comparison of results from predictive models with experimental LLE data for the ternary system (2,4-dimethylphenol + toluene + water) at the temperature  $T = 320$  K and pressure  $p = 0.085$  MPa. ●, this research. The green lines connect the experimental tie-line data of this research, and the blue lines show representative predicted tie lines and the binodal curve computed with the indicated method. Red ◆, LLE composition for the binary system (2,4-dimethylphenol + water) derived with extrapolated LLE temperatures reported by Terres et al.<sup>26</sup> ×, LLE composition for (2,4-dimethylphenol + water) estimated by graphical extrapolation of the ternary results of this research to the binary limit.

Figure 7 and the difficult-to-assess uncertainty in the extrapolations of the ternary data to the binary limit ensure that such a declaration is highly tentative. Additional measurements of LLE for the system (2,4-dimethylphenol + water) are warranted, particularly near room temperature.

#### 4. CONCLUSION

The NIST-modified-UNIFAC and NIST-COSMO-SAC prediction methods were demonstrated, generally, to have good predictive capabilities (within 0.05 mole fraction) for key compound types found in liquid process streams from catalytic fast pyrolysis of biomass. A single exception was found for the

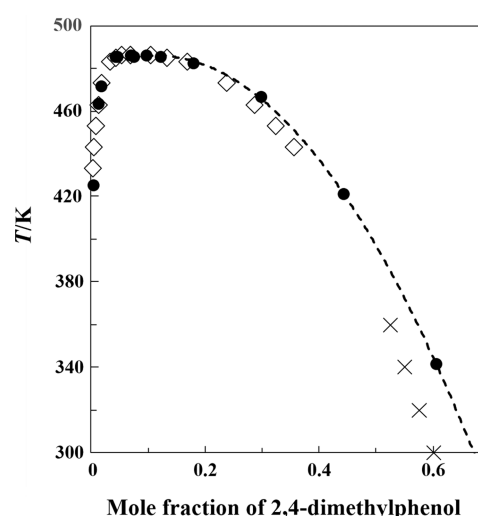


**Figure 7.** LLE temperatures for the system (2,4-dimethylphenol + water) at pressure  $p \sim 0.1$  MPa. ●, experimental values reported by Terres et al.<sup>26</sup> ◊, experimental values reported by Erichsen and Dobbert;  $\cdots$ , curve used for extrapolation to  $T = 300$  K of values reported by Terres et al.<sup>26</sup> ×, LLE conditions estimated in this research by extrapolation of ternary results for (toluene + 2,4-dimethylphenol + water) to zero toluene content. See Figures S21–S24 of the Supporting Information.

system (2-methoxyphenol + water), where prediction with NIST-COSMO-SAC was found to be superior. Intramolecular hydrogen bonding in 2-methoxyphenol was postulated as a possible underlying cause for this result. The presence of such long-range intramolecular interactions are problematic for any group-additivity method. Future work will involve further tests and experimental validation of the predictive models for more complex mixtures of ~8–10 components, as well as additional measurements and testing of predictions for selected model compounds, as needed. Inconsistency in literature results for LLE in the system (2,4-dimethylphenol + water) justify additional measurements for this mixture.

#### ASSOCIATED CONTENT

##### Supporting Information

The Supporting Information is available free of charge on the ACS Publications website at DOI: [10.1021/acs.jcd.6b00625](https://doi.org/10.1021/acs.jcd.6b00625).

(PDF)

#### AUTHOR INFORMATION

##### Corresponding Authors

\*E-mail: [jasperlv@wiltecresearch.com](mailto:jasperlv@wiltecresearch.com) (experimental LLE measurements (Wiltec)).

\*E-mail: [kenneth.kroenlein@nist.gov](mailto:kenneth.kroenlein@nist.gov) (data evaluation and predictive models (NIST)).

\*E-mail: [abhijit.dutta@nrel.gov](mailto:abhijit.dutta@nrel.gov) (program management and CFP analytical chemistry results (NREL)).

##### Funding

This work was supported by the U.S. Department of Energy under Contract No. DE-AC36-08GO28308 with the National Renewable Energy Laboratory. Funding provided by U.S. DOE Office of Energy Efficiency and Renewable Energy, Bioenergy Technologies Office (BETO).

##### Notes

The authors declare no competing financial interest.

## ACKNOWLEDGMENTS

Wiltec Statement: We wish to thank Lane Gardner, who measured the data with precision and meticulous effort. NIST Statement: This article is, in part, a contribution of NIST and is not subject to copyright in the United States for the authors V.D., R.D.C., and K.K. Products or companies are named solely for descriptive clarity, and this neither constitutes nor implies endorsement by NIST or by the U.S. government. Other products may be found to work as well or better.

## REFERENCES

- (1) Mohan, D.; Pittman, C. U.; Steele, P. H. Pyrolysis of Wood/Biomass for Bio-oil: A Critical Review. *Energy Fuels* **2006**, *20*, 848–889.
- (2) Jones, S.; Meyer, P.; Snowden-Swan, L.; Padmaperuma, A.; Tan, E.; Dutta, A.; Jacobson, J.; Cafferty, K. Process Design and Economics for the Conversion of Lignocellulosic Biomass to Hydrocarbon Fuels: Fast Pyrolysis and Hydrotreating Bio-oil Pathway. PNNL-23053; NREL/TP-5100-61178. November 2013. (Available online at [http://www.pnnl.gov/main/publications/external/technical\\_reports/PNNL-23053.pdf](http://www.pnnl.gov/main/publications/external/technical_reports/PNNL-23053.pdf) and <http://www.nrel.gov/docs/fy14osti/61178.pdf>).
- (3) Dutta, A.; Sahir, A.; Tan, E.; Humbird, D.; Snowden-Swan, L.; Meyer, P.; Ross, J.; Sexton, D.; Yap, R.; Lukas, J. Process Design and Economics for the Conversion of Lignocellulosic Biomass to Hydrocarbon Fuels - Thermochemical Research Pathways With In Situ and Ex Situ Upgrading of Fast Pyrolysis Vapors. NREL/TP-5100-62455, PNNL-23823, March 2015. (Available online at <http://www.nrel.gov/docs/fy15osti/62455.pdf> and [http://www.pnnl.gov/main/publications/external/technical\\_reports/PNNL-23823.pdf](http://www.pnnl.gov/main/publications/external/technical_reports/PNNL-23823.pdf)).
- (4) Bozell, J. J.; Petersen, G. R. Technology development for the production of biobased products from biorefinery carbohydrates—the US Department of Energy's "Top 10" revisited. *Green Chem.* **2010**, *12*, 539–554.
- (5) Biddy, M. J.; Scarlata, C.; Kinchin, C. Chemicals from Biomass: A Market Assessment of Bioproducts with Near-Term Potential. NREL/TP-5100-65509, March 2016. (Available online at <http://www.nrel.gov/docs/fy16osti/65509.pdf>).
- (6) Humbird, D.; Davis, R.; Tao, L.; Kinchin, C.; Hsu, D.; Aden, A.; Schoen, P.; Lukas, J.; Olthof, B.; Worley, M. et al. Process Design and Economics for Biochemical Conversion of Lignocellulosic Biomass to Ethanol: Dilute-Acid Pretreatment and Enzymatic Hydrolysis of Corn Stover. NREL/TP-5100-47764. May 2011. (Available online at <http://www.nrel.gov/docs/fy11osti/47764.pdf>).
- (7) Dutta, A.; Talmadge, M.; Hensley, J.; Worley, M.; Dudgeon, D.; Barton, D.; Groendijk, P.; Ferrari, D.; Stears, B.; Searcy, E. M. et al. Process Design and Economics for Conversion of Lignocellulosic Biomass to Ethanol: Thermochemical Pathway by Indirect Gasification and Mixed Alcohol Synthesis. NREL/TP-5100-51400. May 2011. (Available online at <http://www.nrel.gov/docs/fy11osti/51400.pdf>).
- (8) Davis, R.; Tao, L.; Scarlata, C.; Tan, E. C. D.; Ross, J.; Lukas, J.; Sexton, D. Process Design and Economics for the Conversion of Lignocellulosic Biomass to Hydrocarbons: Dilute-Acid and Enzymatic Deconstruction of Biomass to Sugars and Catalytic Conversion of Sugars to Hydrocarbons. NREL/TP-5100-62498. March 2015. (Available online at <http://www.nrel.gov/docs/fy15osti/62498.pdf>).
- (9) Munasinghe, P. C.; Khanal, S. K. Biomass-derived syngas fermentation into biofuels: Opportunities and challenges. *Bioresour. Technol.* **2010**, *101*, 5013–5022.
- (10) Beckham, G. T.; Johnson, C. W.; Karp, E. M.; Salvachua, D.; Vardon, D. R. Opportunities and challenges in biological lignin valorization. *Curr. Opin. Biotechnol.* **2016**, *42*, 40–53.
- (11) Bain, R. L.; Broer, K. Gasification. In *Thermochemical Processing of Biomass: Conversion into Fuels, Chemicals and Power*; Brown, R. C., Ed.; John Wiley & Sons, Ltd: Chichester, United Kingdom, 2011; pp 47–77.
- (12) Bain, R. L.; Magrini-Bair, K. A.; Hensley, J. E.; Jablonski, W. S.; Smith, K. M.; Gaston, K. R.; Yung, M. M. Pilot Scale Production of Mixed Alcohols from Wood. *Ind. Eng. Chem. Res.* **2014**, *53*, 2204–2218.
- (13) Knight, R. Green Gasoline from Wood Using Carbone Gasification and Topsoe TIGAS Processes. Presented at the DOE Bioenergy Technologies Office (BETO) 2015 Project Peer Review, March 24, 2015. (Available online at [http://www.energy.gov/sites/prod/files/2015/04/f22/demonstration\\_market\\_transformation\\_knight\\_3417.pdf](http://www.energy.gov/sites/prod/files/2015/04/f22/demonstration_market_transformation_knight_3417.pdf)).
- (14) Tan, E. C. D.; Talmadge, M.; Dutta, A.; Hensley, J.; Schaidle, J.; Biddy, M.; Humbird, D.; Snowden-Swan, L. J.; Ross, J.; Sexton, D. et al. Process Design and Economics for the Conversion of Lignocellulosic Biomass to Hydrocarbons via Indirect Liquefaction Thermochemical Research Pathway to High-Octane Gasoline Blendstock Through Methanol/Dimethyl Ether Intermediates. NREL/TP-5100-62402; PNNL-23822. March 2015. (Available online at <http://www.nrel.gov/docs/fy15osti/62402.pdf> and [http://www.pnnl.gov/main/publications/external/technical\\_reports/PNNL-23822.pdf](http://www.pnnl.gov/main/publications/external/technical_reports/PNNL-23822.pdf)).
- (15) Hamelinck, C. N.; Faaij, A. P. C.; den Uil, H.; Boerrigter, H. Production of FT transportation fuels from biomass; technical options, process analysis and optimization, and development potential. *Energy* **2004**, *29*, 1743–1771.
- (16) Czernik, S.; Bridgwater, A. V. Overview of Applications of Biomass Fast Pyrolysis Oil. *Energy Fuels* **2004**, *18*, 590–598.
- (17) Liu, C.; Wang, H.; Karim, A. M.; Sun, J.; Wang, Y. Catalytic fast pyrolysis of lignocellulosic biomass. *Chem. Soc. Rev.* **2014**, *43*, 7594–7623.
- (18) Paasikallio, V.; Lindfors, C.; Kuoppala, E.; Solantausta, Y.; Oasmaa, A.; Lehto, J.; Lehtonen, J. Product quality and catalyst deactivation in a four day catalytic fast pyrolysis production run. *Green Chem.* **2014**, *16*, 3549–3559.
- (19) Iliopoulos, E. F.; Stefanidis, S.; Kalogiannis, K.; Psarras, A. C.; Delimitis, A.; Triantafyllidis, K. S.; Lappas, A. A. Pilot-scale validation of Co-ZSM-5 catalyst performance in the catalytic upgrading of biomass pyrolysis vapours. *Green Chem.* **2014**, *16*, 662–674.
- (20) Dutta, A.; Schaidle, J. A.; Humbird, D.; Baddour, F. G.; Sahir, A. Conceptual Process Design and Techno-Economic Assessment of Ex Situ Catalytic Fast Pyrolysis of Biomass: A Fixed Bed Reactor Implementation Scenario for Future Feasibility. *Top. Catal.* **2016**, *59*, 2–18.
- (21) Pakdel, H.; Piskorz, J.; Himmelblau, A.; Clements, D. Workshop on Chemicals from Biomass. In *Developments in Thermochemical Biomass Conversion Vol. 1/Vol.2*; Bridgwater, A. V., Boocock, D. G. B., Eds.; Springer Science + Business Media: Dordrecht, The Netherlands, 1997; pp 1621–1625.
- (22) Oasmaa, A.; Peacocke, C. Properties and Fuel Use of Biomass Derived Fast Pyrolysis Liquids: A Guide. VTT Technical Research Centre of Finland, Ltd, VTT Publication 731, VTT, Finland. 2010. (Available online at <http://www.vtt.fi/Documents/P731.pdf>).
- (23) Mukarakate, C.; Zhang, X.; Stanton, A. R.; Robichaud, D. J.; Ciesielski, P. N.; Malhotra, K.; Donohoe, B. S.; Gjersing, E.; Evans, R. J.; Heroux, D. S.; et al. Real-time monitoring of the deactivation of HZSM-5 during upgrading of pine pyrolysis vapors. *Green Chem.* **2014**, *16*, 1444–1461.
- (24) Engtrakul, C.; Mukarakate, C.; Starace, A. K.; Magrini, K. A.; Rogers, A. K.; Yung, M. M. Effect of ZSM-5 acidity on aromatic product selectivity during upgrading of pine pyrolysis vapors. *Catal. Today* **2016**, *269*, 175–181.
- (25) Iisa, K.; French, R. J.; Orton, K. A.; Yung, M. M.; Johnson, D. K.; ten Dam, J.; Watson, M. J.; Nimlos, M. R. In Situ and ex Situ Catalytic Pyrolysis of Pine in a Bench-Scale Fluidized Bed Reactor System. *Energy Fuels* **2016**, *30*, 2144–2157.
- (26) Terres, E.; Gebert, F.; Hulsemann, H.; Petereit, H.; Toepsch, H.; Ruppert, W. Phenol Components of Tar. VI. Investigation of Monohydroxyphenol-water Systems and Their Critical Solution Temperatures. *Brennst.-Chem.* **1955**, *36*, 289–301.
- (27) Maczynski, A.; Shaw, D. G.; Goral, M.; Wisniewska-Gocłowska, B.; Skrzecz, A.; Owczarek, I.; Blazej, K.; Haulait-Pirson, M.-C.; Hefter, G. T.; Kapuku, F.; et al. IUPAC-NIST solubility data series. 81. Hydrocarbons with water and seawater-revised and updated. Part 5.

C7 hydrocarbons with water and heavy water. *J. Phys. Chem. Ref. Data* **2005**, *34*, 1399–1487.

(28) Erichsen, L. V.; Dobbert, E. The reciprocal relation of solubility of alkylphenols and water. *Brennst.-Chem.* **1955**, *36*, 338–345.

(29) Hooper, H. H.; Michel, S.; Prausnitz, J. M. High-temperature mutual solubilities for some binary and ternary aqueous mixtures containing aromatic and chlorinated hydrocarbons. *J. Chem. Eng. Data* **1988**, *33*, 502–505.

(30) Mohsen-Nia, M.; Paikar, I. Ternary and Quaternary Liquid + Liquid Equilibria for Systems of (Water + Toluene + m-Xylene + Phenol). *J. Chem. Eng. Data* **2007**, *52*, 180–183.

(31) Martin, A.; Klauck, M.; Taubert, K.; Precht, A.; Meinhardt, R.; Schmelzer, J. Liquid-Liquid Equilibria in Ternary Systems of Aromatic Hydrocarbons (Toluene or Ethylbenzene) + Phenols + Water. *J. Chem. Eng. Data* **2011**, *56*, 733–740.

(32) Paulechka, E.; Diky, V.; Kazakov, A.; Kroenlein, K.; Frenkel, M. Reparameterization of COSMO-SAC for Phase Equilibrium Properties Based on Critically Evaluated Data. *J. Chem. Eng. Data* **2015**, *60*, 3554–3561.

(33) Kang, J. W.; Diky, V.; Frenkel, M. New modified UNIFAC parameters using critically evaluated phase equilibrium data. *Fluid Phase Equilib.* **2015**, *388*, 128–141.

(34) Klamt, A. Conductor-like screening model for real solvents: a new approach to the quantitative calculation of solvation phenomena. *J. Phys. Chem.* **1995**, *99*, 2224–2235.

(35) Klamt, A.; Jonas, V.; Burger, T.; Lohrenz, J. C. W. Refinement and Parametrization of COSMO-RS. *J. Phys. Chem. A* **1998**, *102*, 5074–5085.

(36) Grensemann, H.; Gmehling, J. Performance of a Conductor-like Screening Model for Real Solvents in Comparison to Classical Group Contribution Methods. *Ind. Eng. Chem. Res.* **2005**, *44*, 1610–1624.

(37) Pye, C. E.; Ziegler, T.; van Lenthe, E.; Louwen, J. N. An implementation of the conductor-like screening model of solvation within the Amsterdam density functional package – Part II. COSMO for real solvents. *Can. J. Chem.* **2009**, *87*, 790–797.

(38) Lin, S. T.; Sandler, S. I. A Priori Phase Equilibrium Prediction from a Segment Contribution Solvation Model. *Ind. Eng. Chem. Res.* **2002**, *41*, 899–913.

(39) Gutierrez-Sevillano, J. J.; Leonhard, K.; van der Eerden, J. P. J. M.; Vlugt, T. J. H.; Krooshof, G. J. P. COSMO-3D: Incorporating Three-Dimensional Contact Information into the COSMO-SAC Model. *Ind. Eng. Chem. Res.* **2015**, *54*, 2214–2226.

(40) Mu, T.; Rarey, J.; Gmehling, J. Performance of COSMO-RS with Sigma Profiles from Different Model Chemistries. *Ind. Eng. Chem. Res.* **2007**, *46*, 6612–6629.

(41) Constantinescu, D.; Rarey, J.; Gmehling, J. Application of COSMO-RS Type Models to the Prediction of Excess Enthalpies. *Ind. Eng. Chem. Res.* **2009**, *48*, 8710–8725.

(42) Weidlich, U.; Gmehling, J. A modified UNIFAC model. 1. Prediction of VLE, hE, and  $\gamma^\infty$ . *Ind. Eng. Chem. Res.* **1987**, *26*, 1372–1381.

(43) Gmehling, J.; Li, J.; Schiller, M. A modified UNIFAC model. 2. Present parameter matrix and results for different thermodynamic properties. *Ind. Eng. Chem. Res.* **1993**, *32*, 178–193.

(44) Gmehling, J.; Lohmann, J.; Jakob, A.; Li, J.; Joh, R. A Modified UNIFAC (Dortmund) Model. 3. Revision and Extension. *Ind. Eng. Chem. Res.* **1998**, *37*, 4876–4882.

(45) Gmehling, J.; Wittig, R.; Lohmann, J.; Joh, R. A Modified UNIFAC (Dortmund) Model. 4. Revision and Extension. *Ind. Eng. Chem. Res.* **2002**, *41*, 1678–1688.

(46) Jakob, A.; Grensemann, H.; Lohmann, J.; Gmehling, J. Further Development of Modified UNIFAC (Dortmund): Revision and Extension 5. *Ind. Eng. Chem. Res.* **2006**, *45*, 7924–7933.

(47) Goral, M.; Shaw, D. G.; Maczynski, A.; Wisniewska-Gocłowska, B. IUPAC-NIST solubility data series. 91. Phenols with Water. Part 1. C6 and C7 Phenols with Water and Heavy Water. *J. Phys. Chem. Ref. Data* **2011**, *40*, 033102.